Improved Direct Torque Control of Axial-Flux Hysteresis Motor

Saman Amini [1], Abolfazl Halvaei Niasar [2], Keyvan Amini [3]
1- Department of Electrical & Computer Eng. of Kashan University, Kashan, Iran.
Email: SamanAmini24@outlook.com (Corresponding author)
2- Department of Electrical & Computer Eng. of Kashan University, Kashan, Iran.
Email: Halvaei@kashan.ac.ir
3- Department of Electrical & Computer Eng. of Tabriz University, Tabriz, Iran.
Email: k.amini@outlook.com

Received: May 2018 Revised: June 2018 Accepted: July 2018

ABSTRACT:
In this study an improved direct torque control method (DTC) for Axial-flux hysteresis motor speed controlling is investigated. Time-consuming and dangerously of the necessity to manually adjust the motor speed and voltage when motor lagging occurs are the main drawback of the conventional control methods. The proposed method under acceleration and sequential braking on the Axial-flux hysteresis motor, based on the extracted modified motor dynamic equations in the Simulink Matlab environment has been simulated. As the results show, by using the proposed direct torque control method, the speed of the motor in the consecutive acceleration and braking process is controlled and the referral speed throughout the process operation with high accurate has been followed. Also this control system has shown that it is reliable method and stable against disturbances. Compared with conventional vector control methods, less complexity, higher speed and accuracy and easier implementation ability are significant features of the proposed method.

KEYWORDS: Axial-flux hysteresis motor; Dynamic model; SVM- DTC; Direct torque control.

1. INTRODUCTION

Hysteresis motors are classified as synchronous motors. the simplicity of work, notable startup torque and the constant speed at the synchronous speed are the most significant features of the hysteresis motor. These motors are used extensively in high-speed applications such as centrifuges and gyroscopes. On the other hand, due to having a constant hysteresis torque, throughout the rotor startup period of the hysteresis motor revolves smoothly over a period of operation. Also because of the nature of induced hysteresis losses caused by the initial battalion in the hysteresis magnetic, and by the secondary magnetic residual, rotate with synchronization speed.

The structure of the hysteresis motor is similar to the structure of the squirrel cage induction motors. The stator is equipped with a three-phase sinusoidal distributed winding, and the main part of the rotor is fabricated from semi-hard magnetic materials such as cobalt, vanadium, iron-cast alloys. The magnetic material of the rotor can be either rigid material or made of torsional magnetic film foils.

In today's conventional structures, at the final speed and in order to reduce the number of electric motor losses and reduce the temperature, the inverter output voltage decreases significantly in manual mode and the motor voltage must be reset to make any change in the speed. Thus, when lagging occur at the motor, which can be caused by overload or interruption of the power supply of the inverter, the operator has to measure the actual speed of the motor and manually adjust the voltage and frequency of the inverter output. This is a time-consuming and risky method, and it's dangerous when it happens at the same time for several motors. By using the closed-loop motor controlling method, the mentioned problem and risks will be eliminated.

Hysteresis motors are divided into two axial-flux (or disc-based) and radial-flux (or cylindrical) in terms of the direction of airflow.

This study is dedicated to controlling axial-flux motors. Because of their smaller size and less weight, the core of these motors has a higher power density than cylindrical ones. These motors can be designed as two-way, one-way or even multi-discipline. Axial-flux hysteresis motors also have valuable characteristics, such as high volumetric density, high torque and high-efficiency ratio, which are used in high-speed applications where space-limitation and interest-rate are very important. Also, the volumetric torque is high due

to the larger air distance, which provides more space for magnetic responses.

2. THE DYNAMIC MODEL OF THE HYSTRESIS MOTOR

Most of the electrical motor classic control methods require a dynamic model, as instances like vector control, direct torque control, and methods based on control theories such as slip mode controller, feedback linearization, and reference model controller. In the hysteresis motor, the dynamic model is more complicated due to the difficulty of the rotor magnetic ring modeling.

2.1. An overview of the hysteresis motor's dynamic models

The major difference between the permanent magnet synchronous motor and the hysteresis motor is in the modeling of magnetic material [1, 2]. The PMHS motor is the same as the hysteresis motor, with the difference that its rotor has a hysterical material such as steel-cobalt 36%, with a permanent magnet [3]. The transient behavior and steady state of this motor are examined in [4, 5], by using the dynamic model obtained from the analytical methods. Fig. 1 shows the equivalent circuit of the basic hysteresis motor dynamic model in the qd0 two-axis system. The hysteresis material of the rotor is also modeled with a constant Rh resistance in both d and q axes. Foucault's losses are also modeled with constant resistance (Re) on both axes. Some other researches on the hysteresis motor dynamic modeling are published in [6, 7, and 8]. At [7] by modifying the model that presented in [6], transient state behaviors on motor behavior, such as the effect of stator voltage and step load variations has been studied.

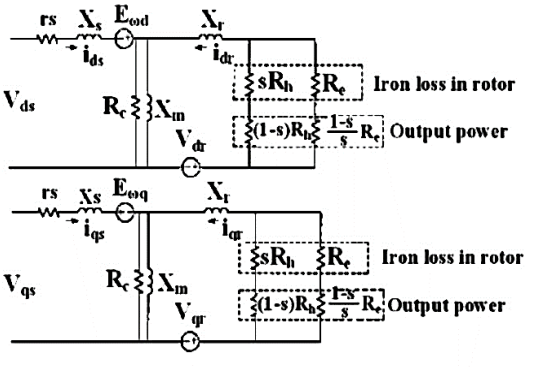

Fig.1. Dynamic model of the PMHS motor at qd0 coordinate system [6],[7]

Another axial-flux hysteresis motor model is proposed based on the [9], in which the drawbacks of the presented model in [6] have been solved. The resistance of the hysteresis ring in this study is dependent on the hysteresis curve and the amount of resistance varies with the curve changing [7-10].

2.2. Dynamic model of the hysteresis motor

In this part, a mathematical model based on the electrical and mechanical quantities of the motor is obtained to predict the behavior of the hysteresis motor under various load and speed conditions. In the hysteresis motor, there is no winding on the rotor but similar to the squirrel cage induction motor modeling, corresponding to the three-phase stator winding. three hypotheticals short-circuit coils can also be considered on the rotor. Therefore, the dynamic model of the hysteresis motor is very similar to the induction motor with this difference that the rotor resistance at any moment in time depends on the speed, slip and the air gap flux.

The voltage applied to each of the six coils will be the sum of the drop an ohmic loss and an $d\lambda/dt$ expression. The voltage equations for the stator and rotor windings can be arranged in the following way:

$$\begin{bmatrix} V_s^{abc} \\ V_r^{abc} \end{bmatrix} = \begin{bmatrix} r_s^{abc} & 0 \\ 0 & r_r^{abc} \end{bmatrix} \begin{bmatrix} r_s^{abc} \\ r_r^{abc} \end{bmatrix} + \frac{d}{dt} \begin{bmatrix} \lambda_s^{abc} \\ \lambda_r^{abc} \end{bmatrix} \quad (1)$$

$$\begin{bmatrix} \lambda_s^{abc} \\ \lambda_r^{abc} \end{bmatrix} = \begin{bmatrix} L_{ss}^{abc} & L_{sr}^{abc} \\ L_{rs}^{abc} & L_{rr}^{abc} \end{bmatrix} \begin{bmatrix} i_s^{abc} \\ i_r^{abc} \end{bmatrix} \quad (2)$$

In the above equations, V_s^{abc} and V_r^{abc} are the rotor and stator voltage vectors, i_s^{abc} and i_r^{abc} are the rotor and stator current vectors, λ_s^{abc} and λ_r^{abc} are the stator and rotor linked-flux vector.

In most of the offered models for hysteresis motors due to the uniformity of the air gap in the hysteresis motor, by ignoring the magnetic resistivity of the iron, the inductances of the above questions can be defined in terms of the number of stator windings turns (N_s) and the rotor winding turns (N_r) and the magnetic conductivity of the air distance (P_g). But this assumption is not correct for the hysteresis motor. By using the following transformation matrix, to transfer the abc coordinate system quantities to a dual-axis qd system, the stator and rotor voltage equations on the qd system will be obtained (Eq. 3 & 4).

$$\begin{bmatrix} V_{qs} \\ V_{ds} \\ V_{os} \end{bmatrix} = \omega_r \begin{bmatrix} 0 & 1 & 0 \\ -1 & 0 & 0 \\ 0 & 0 & 0 \end{bmatrix} \begin{bmatrix} \lambda_{qs} \\ \lambda_{ds} \\ \lambda_{os} \end{bmatrix} + \frac{d}{dt} \begin{bmatrix} \lambda_{qs} \\ \lambda_{ds} \\ \lambda_{os} \end{bmatrix} + r_s \begin{bmatrix} i_{qs} \\ i_{ds} \\ i_{os} \end{bmatrix} \quad (3)$$

$$\begin{bmatrix} V'_{qr} \\ V'_{dr} \\ V'_{or} \end{bmatrix} = + \frac{d}{dt} \begin{bmatrix} \lambda'_{qr} \\ \lambda'_{dr} \\ \lambda'_{or} \end{bmatrix} + r'_r \begin{bmatrix} i'_{qr} \\ i'_{dr} \\ i'_{or} \end{bmatrix} \quad (4)$$

The prime sign, in the above matrix equations, represents the transfer of a quantity from the rotor circuit to the stator. Fig. 2 shows the equivalent hysteresis motor circuit represents the qd rotating reference system that linked to the rotor. The linkage flux of the stator and rotor in the dq reference coordinate system is obtained by applying dq to abc transformation matrix. Which after simplification will be obtained as Eq. (5).

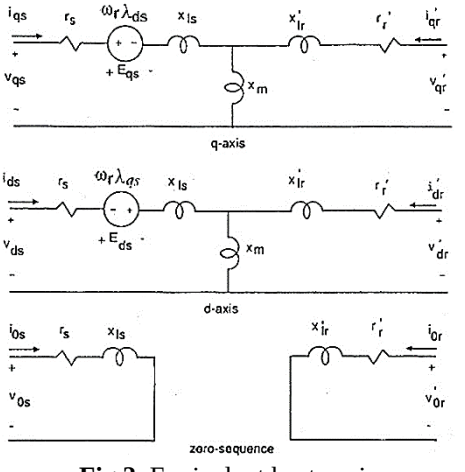

Fig.2. Equivalent hysteresis motor circuit, in the rotor-connected qd rotary coordinate system

$$\begin{bmatrix} \lambda_{qs} \\ \lambda_{ds} \\ \lambda_{os} \\ \lambda'_{qr} \\ \lambda'_{dr} \\ \lambda'_{or} \end{bmatrix} = \begin{bmatrix} L_{1s}+L_m & 0 & 0 & L_m & 0 & 0 \\ 0 & L_{1s}+L_m & 0 & 0 & L_m & 0 \\ 0 & 0 & L_{1s}+L_m & 0 & 0 & 0 \\ L_m & 0 & 0 & L'_{1r}+L_m & 0 & 0 \\ 0 & L_m & 0 & 0 & L'_{1r}+L_m & 0 \\ 0 & 0 & 0 & 0 & 0 & L'_{1r} \end{bmatrix} \times \begin{bmatrix} i_{qs} \\ i_{ds} \\ i_{os} \\ i'_{qr} \\ i'_{dr} \\ i'_{or} \end{bmatrix} \quad (5)$$

The electromagnetic torque produced by the motor is also obtained by using the power equations in the qd coordinate system and by ignoring the power losses of copper and stored-power in the magnetic field. Instead of the quantity of linked-flux (λ) and the inductance (L), it can be used the linked-flux quantity based on the time or flux per second (Ψ) and reactance (x). These quantities are obtained simply by multiplying the base angular speed in the linked-flux and the inductance Eq. (6).

$$T_{em} = \frac{3}{2} \frac{P}{2\omega_b} (\psi_{ds} i_{qs} - \psi_{qs} i_{ds}) \quad (6)$$

3. DIRECT TORQUE CONTROL THEORY

The electric motors frequency controlling methods can be divided into two general categories of scalar and vector control methods. Vector control method is one of indirect torque and flux controlling method with two current control loops. Along with dq coordinate system conversions and the reversal of this transformation will create a large computational volume. High computing value, requiring a powerful processor, the complexity of the method and the large control loops setup setting have led researchers looking for direct torque control methods without current controlling, instead of indirectly torque and flux controlling.

Over two decades since the introduction of the theory of direct torque control, various strategies have been developed. The proposed strategies in terms of the inverter switching frequency are divided into two categories; Variable switching frequency and Static switches with constant frequency switching strategies. Variable switching frequency strategies that are more ancient, are based on the switching table and direct control (known as the DTC). Finding new method to constant the inverter switching frequency is essential, Due to the switching frequency is unpredictable and variable with the load conditions and it is considered as a weakness of the direct torque control strategy. The most notable new methods are direct torque control with variable hysteresis bands, Direct Torque Control with Spatial Vector Modulation Inverter (SVM) and direct torque control with predictive models. However, these methods are able to solve the variable frequency issue of the inverter switching but instead, due to the using more sophisticated control methods, the simplicity of variable frequency methods which was the main feature of direct torque control, will be lost.

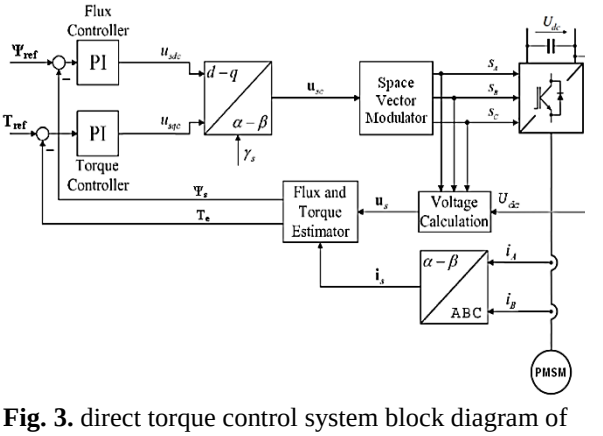

Fig. 3. direct torque control system block diagram of the PMSM motor with the SVM-DTC method.

3.1. Direct torque control of PMSM motor by the DTC-SVM method.

Fig. 3 shows the block diagram of the SVM-DTC control method. In this scheme, the flux and torque error are passed through two PI controllers and the stator voltage control signals are generated. Subsequently, the vector space modulator base on the amplitude and phase of the stator voltage vector, generates the necessary commands for the inverter switches. By using the PI

controller results, the flux and torque steady-state error will be zero and the flux and torque fluctuations during the changing from one sector to another are also eliminated. In order to eliminate the effects of d-and q-axis voltage interference on each other and improve the dynamic performance of the torque controller, Voltage decoupling can be used and the component ($\omega\psi_S$) can be added to the torque controller output.

The performance of the DTC designs can be improved. This improvement, especially for the DTC-ST method is more tangible due to at voltage vector choosing cannot be differentiated between large and small errors of the flux and torque. Some studies proposed the DTC method based on 12 spatial sectors instead of the 6-classical sector mode. In the classical six-sector method, there are two voltage vectors in each sector who their impact on torque is ambiguous. Therefore, they are not used commonly. For example, in the first sector, vectors V1 and V4 increase the torque in one half-sector of 33 degrees and reduce the torque by another 33 degrees in the same sector. Therefore, the performance appears to be improved if the 360-degree vector space is divided into 12 parts by 30 degrees instead of six 60-degree sections. By shrinking the sectors, achieving the reference torque in each sector is done better due to the torque error is divided into smaller areas. Fig. 4 shows the twelve mentioned sectors.

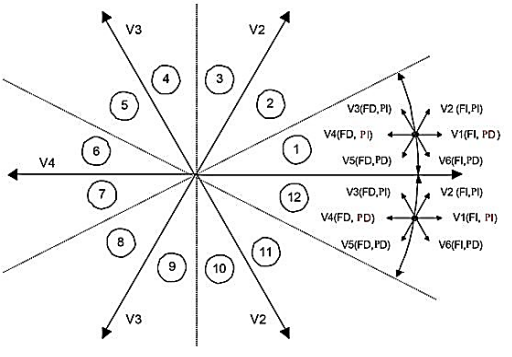

Fig. 4. Twelve-sector vector space in DTC method

4. SIMULATION RESULTS

The SVM-DTC control method is widely used in the motor speed controlling, due to its high potential benefits such as low waveform distortion, high voltage DC utilization, analog-to-digital execution, the constant frequency of switching inverter, torque fluctuation Reduction and motor-linked flux.

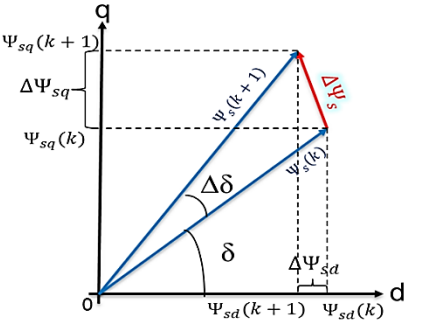

Fig.5. Stator flux vector to estimate SVM voltage vectors

The used control method in this study is combination of three methods of speed closed-loop control linkage flux and linkage torque. In the hysteresis motor DTC method the $i_{s\alpha}$ and $i_{s\beta}$ and components of i_s in the $\alpha\beta$ coordinates system can be obtained by sampling the current phases of i_a, i_b, i_c. Thus, ϕ_{sd} and ϕ_{sq} can be estimated by using Clark's transformation into Park transformation and by using $i_{sa}, i_{s\beta}$ also by sampling the voltage of the phases and the position of the rotor. The stator flux in the static coordinate system and the electromagnetic torque (T_e) can be calculated from the following equations (7, 8 and 9):

$$\phi_{sa} = \int (v_{sa} - r_s i_{sa})dt \quad (7)$$

$$\phi_{s\beta} = \int (v_{s\beta} - r_s i_{s\beta})dt \quad (8)$$

$$T_e = \frac{3P}{4}(\phi_{sa} i_{s\beta} - \phi_{s\beta} i_{sa}) \quad (9)$$

By considering changes in the speed of $\Delta\omega_r$ as input value, the reference torque value (T^*_{e-ref}) of the PI controller outer ring output, can be achieved, which gives the ring torque value. also, ΔT_e is considered as the PI controller input. The variations of the $d\delta$ obtained from the output of the PI close-loop controller, that is modified parameter of the δ (the angle between the stator flux and the rotor). Voltage vectors of u_{sd} and u_{sq} and u_s in the dq coordinate system can be estimated by using $d\delta$, $d\psi_{sd}$ and $d\psi_{sq}$. According to Fig. 5 (dt is the flux linking sampling time), ψ^*_s gives the stator flux- linked variations. By assuming that the motor is controlled by a control system over a period of time, the flux and the angle of flux are considered to be $\psi_s(k)$ and $\delta(k)$ respectively. After a period of control, the value of stator flux is equal to $\psi_s(k+1)$ and the angle is equal to $\delta(k+1)$.

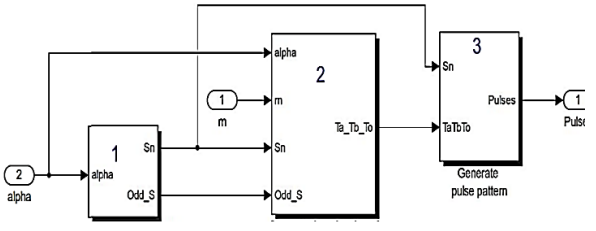

Fig. 6. SVM block components

Also by assuming that in one control period the flux value is equal to the value of the stator reference flux, it can be considered that $\psi_s^* = \psi_s(k+1)$, so due to motor equations the estimation of the reference voltage vector will be:

$$d\psi_{sd} = \psi_s^*\left(\frac{\psi_{sd}}{|\psi_s|}\mathrm{Cos}(d\delta) - \frac{\psi_{sq}}{|\psi_s|}\mathrm{Sin}(d\delta)\right) - \psi_{sd} \quad (10)$$

$$d\psi_{sq} = \psi_s^*\left(\frac{\psi_{sq}}{|\psi_s|}\mathrm{Cos}(d\delta) - \frac{\psi_{sd}}{|\psi_s|}\mathrm{Sin}(d\delta)\right) - \psi_{sq} \quad (11)$$

At Eq. (10 and 11), ψ_s^* is reference Linked-Flux of the stator and ψ_s is actual stator flux value of the hysteresis motor. By using the Park reverse converter, u_{sd} and u_{sq} have been converted to $u_{s\alpha}$ and $u_{s\beta}$ Eq. (12, 13).

$$u_{sd} = R_s i_{sd} + \frac{d\psi_{sd}}{dt} - \omega_r \psi_{sq} \quad (12)$$

$$u_{sq} = R_s i_{sq} + \frac{d\psi_{sq}}{dt} - \omega_r \psi_{sd} \quad (13)$$

After calculating $u_{s\alpha}$ and $u_{s\beta}$, the obtained voltage vectors are applied to SVPWM block to generating control pulses in order to feed the motor. The SVPWM block is shown in Fig. (6). Voltages $u_{s\alpha}$ and $u_{s\beta}$ are used as input to determine the reference voltage vector (U^*). Therefore the angle of α (the angle between the reference voltage vector and basic space vector) and coefficient of modulation (m) can be achieved. The input of the space vector modulation block is m and α. By controlling the printing frequency, the control command is sent to the inverter for switching operation. In the block 1 shown in Fig. 6, based on the angle of the α, the sector of the reference voltage vector is determined. In block 2, the times of the T_0, T_1, T_2 are determined. The input of the block 3 is the signal vectors of T_0, T_1, T_2 and the sector of the voltage vector (Sn). According to above vectors, the inverter's switching pulse pattern is generated and given to the input of the inverter gate in order to be done the switching operation in the inverter and control the hysteresis motor in acceleration and permanent operation modes.

4.1. Line-starting axial-flux hysteresis motor under load with nominal voltage and frequency.

In this simulation, the load torque is assumed to be $T_{load} = T_0 + B_f \omega^2$, while its constant value assumed to be zero. The value of B_f is chosen so that the load torque at the nominal speed is equal to 1 pu. Fig. 7 shows the stator flux at start-up with direct torque control and Fig. 8 shows the changing in the electromagnetic torque and load and in Fig. 9 momentary variations of motor speed is shown. The motor under load, after passing through the transient state, reaches the speed of 1 pu at the frequency of 1000 Hz. Both of the speed and torque value oscillated due to changing the switching speed at high frequency.

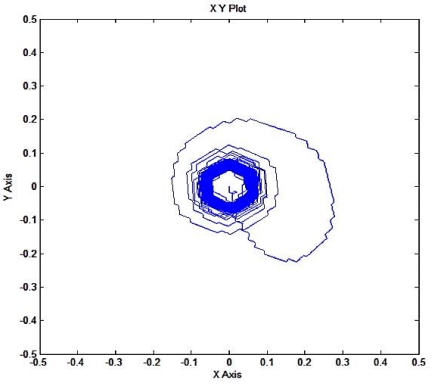

Fig. 7. The dq components of stator flux in direct torque control method

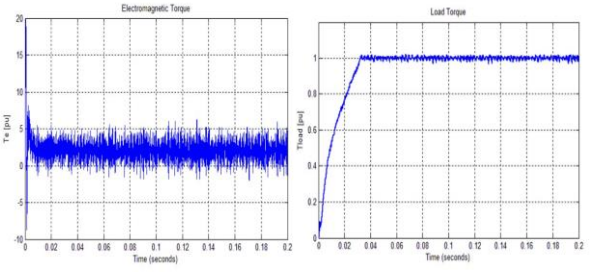

Fig.8. Electromagnetic and load torque of the hysteresis motor with applying nominal voltage and frequency.

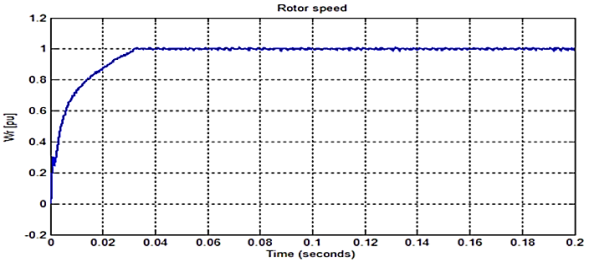

Fig. 9. Speed variations of the axial-flux hysteresis motor by applying nominal voltage and frequency.

The created value of torque in a permanent state varies around an approximate of 1 pu value. The torque also varies with the squared of the speed.

4.2. Load variations

The effect of applying the constant load torque on motor behavior during the working period is investigated. As shown in Fig. 10, the load torque and especially its fixed part, alternately changes (T_0 & T_{load}). The fixed part of the load torque, at synchronous speed changes in the form of a pulse. Fig. 11 shows the variation in the speed of the hysteresis motor. By increasing or decreasing the torque of the load, after passing the transient state, the speed of synchronization is maintained.

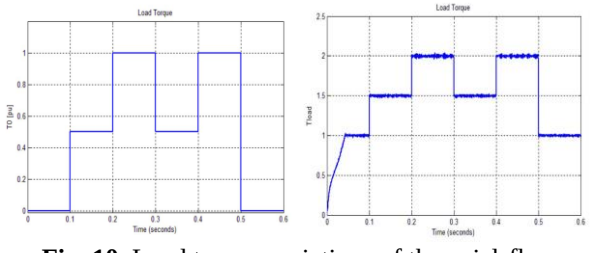

Fig. 10. Load torque variations of the axial-flux hysteresis motor at synchronous speed (T_0 & T_{load}).

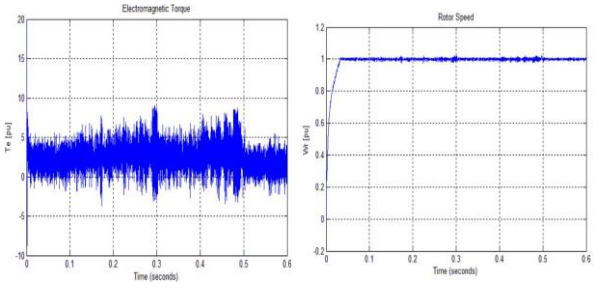

Fig. 11. Electromagnetic torque and speed variations of axial-flux hysteresis motor at synchronous speed.

4.3. Start-up motor by closed-loop direct control of the torque -SVM-DTC

Fig. 12 shows the variations of the frequency, speed, electromechanical and load torque. Its value gradually reaches to the nominal value. It is observed that the speed tracking error is negligible with the exception of the simulation initial moment, the motor has followed the reference frequency.

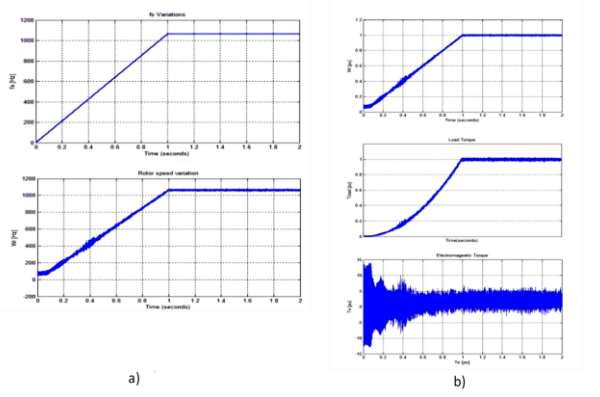

Fig.12. a) The frequency of the speed, b) the electromagnetic and load torque variations of the hysteresis motor at start-up by using DTC method.

5. COMCLUSION

In this study, the DTC control strategy, based on the SVM technique, has been used. The focus of this study is in direct control of the flux-based, single-disc motor and its dynamic model. The direct torque control method is implemented on the axial-flux hysteresis motor. The proposed control system is much less complex and faster than the other vector control method.

According to the obtained results, in the design and simulation of the direct control closed-loop method of the hysteresis motor torque and in accordance with the scalar control structure for the hysteresis motor at the final speed and in order to reduce the motor's electrical losses and temperature, the inverter output voltage is manually significantly decreases and to change the speed, the motor voltage must be re-setup. The SVM-DTC method can overcome the problems caused by motor speed retardation and functional insecurity. By using the DTC method, the reference speed followed with high precision. these results are valid for the acceleration and consecutive braking operations. The control system showed that it is highly stable against distortions and in the critical condition this method is reliable.

REFERENCES

[1] .C.P. Steinmentz; **"*Theory and Calculation of Electrical Apparatus*",** *Mac Graw -Hill,* New York, 1917

[2] J. Qian; **"*Microprocessor implementation of field oriented control for permanent magnet hysteresis synchronous motor*",** *M.S. Thesis, Memorial University of Newfoundland,* 1990.

[3] M.A. Rahman, R. Qin; **"Starting and Synchronization of Permanent Magnet Hysteresis Motors",** *IEEE Trans. on Indus App,* Vol. 32, No. 5, Sep./Oct. 1996.

[4] A. Darabi, M. Hossein Sadeghi, and A. Hassannia, **"Design Optimization of Multistack Coreless Disk-Type Hysteresis Motor"**, *IEEE Trans. on Energy Conversion*, Vol. 26, No. 4, pp. 1081-1087, Dec. 2011.

[5] A. Halvaei Niasar, H. Moghbelli, **"Sensitivity Analysis to the Design Parameters of a Hysteresis Motor,"** *in Proceedings of the 3rd IEEE Power Elec, Drive Syst & Tech Conference (PEDSTC 2012),* 2012, pp. 73-77.

[6] M.A. Rahmani, A.M. Osheiba; **"Dynamic Performance Prediction of Poly Phase Hysteresis Motors",** *IEEE Trans. on Indus App*, Vol. 26, No.6, pp. 1026-1033, November 1990.

[7] A. Darabi, T. Ghanbari, M. Rafiei, H. Lesani, M. Sanati-Moghadam; **"Dynamic Performance Analysis of Hysteresis Motors by a Linear Time-Varying Model",** *Iranian Journal of Electrical & Electronic Engineering*, Vol. 4, No. 4, October 2008, pp. 202-215.

[8] M.A. Rahmani, A.M. Osheiba; **"Dynamic Performance Prediction of Hysteresis Motors",** *IEEE Indus App Society Annual Meeting*, 1989, Vol. 1, pp. 278-284.

[9] A.M. Trzynadlowski; **"The Field Orientation Principle in Control of Induction Motors",** *Kluwer Academic Publishers*, p. 255, 1994.

[10] R. Krishnan, "**Permanent Magnet Synchronous and Brushless dc Motor Drives",** Taylor and Francis Group, LLC, 2010.